LOW COMPLEXITY AZIMUTH AND ELEVATION ESTIMATION FOR ARBITRARY ARRAY CONFIGURATIONS

Mário Costa, Visa Koivunen[*]

Helsinki University of Technology
Department of Signal Processing and Acoustics, SMARAD CoE
P.O. Box 3000, FIN-02015 TKK, Finland
Email: {forename.surname}@hut.fi

Andreas Richter[†]

Nokia Research Center,
P.O.Box 407, FIN-00045 NOKIA GROUP, Finland
Email: {forename.surname}@nokia.com

ABSTRACT

In this paper we propose azimuth and elevation angle of arrival estimation algorithms for arbitrary array configurations. The proposed algorithms extend the Polynomial Rooting Intersection for Multidimensional Estimation (PRIME) [1] and statistically efficient Modified Variable Projection (MVP) [2] algorithms to arbitrary sensor array configurations without explicit knowledge of the steering vector. The proposed algorithms exploit the concept of Manifold Separation Technique (MST) [3], [4]. Thus, the data are processed in the element-space domain and are not subject to mapping errors. Moreover, closed-form derivatives of the Weighted Subspace Fitting (WSF) cost function are obtained, even for real-world arrays with imperfections, making the proposed MVP computationally attractive. The obtained estimates for both elevation and azimuth show an error variance close to the Cramér-Rao Lower Bound (CRLB).

Index Terms— DoA estimation, WSF, polynomial rooting, arbitrary arrays, array calibration measurements.

I. INTRODUCTION

In array signal processing it is often convenient to use regular sensor array geometries such as Uniform Planar Arrays (UPAs). This leads to reduced computation since the steering vector matrix can be obtained from two Vandermonde structured matrices. Hence, computationally efficient high-resolution 2-D Direction-of-Arrival (DoA) estimation algorithms such as RARE [5] and PRIME [1] may be employed. Moreover, the statistically efficient 2-D MODE [6] can also be applied to UPAs by exploiting such a structure in the steering vectors.

In cases where the geometry of the sensor array is arbitrary or the steering vector is not known explicitly (array calibration measurements), the aforementioned algorithms can only be used after a pre-processing of the data by an array interpolation technique [7]. However, the mapping of the data introduces errors in the form of bias and excess variance since e.g. the Vandermonde structure is obtained only approximately. Consequently, the acquired DoA estimates may be far from optimal.

In this paper, we propose novel algorithms for azimuth and elevation estimation that extend the computationally efficient PRIME [1] and the statistically efficient MVP [2] to arbitrary sensor array configurations (possibly with imperfections). Additionally, the proposed estimators were derived based on array calibration measurements, making them suitable for real-world arrays. The proposed extension of the PRIME algorithm avoids the high complexity search-based algorithms e.g. 2-D MUSIC since the DoA estimates are obtained by polynomial rooting. Moreover, the proposed MVP is computational attractive wrt the conventional MVP since closed-form derivatives of the WSF cost function and Vandermonde structured vectors for the unknown parameter, are obtained for arbitrary array configurations with imperfections (similarly to real-world arrays). The proposed algorithms exploit the Manifold Separation Technique (MST) [3]. In particular, the element-space steering vector of an arbitrary sensor array configuration is modelled as the product of a sampling matrix that depends only on the sensor array configuration and two Vandermonde structured vectors that depends on the wavefield. Unlike the array interpolation techniques, it does not require sector-by-sector processing. Instead, the whole 2-D visible region is modelled. In theory, the modelling errors can be made as small as desired [3], [4].

This paper is organized as follows. In Section II, the signal and array models are presented. In Section III, an extension of the MST is given. In Section IV, we show that the 2-D MUSIC cost function using MST can be represented as a bivariate polynomial. In Section V, the proposed ES-PRIME algorithm for joint azimuth and elevation estimation on arbitrary array configurations is derived. In Section VI, the proposed extension of the MVP is derived. In Section VII, the statistical performance of the algorithms is illustrated by simulations. Finally, Section VIII concludes the paper.

II. SIGNAL AND ARRAY MODELS

Consider that $P (P < N)$ incoherent narrowband signal sources impinge a sensor array of N-sensors from directions $(\boldsymbol{\theta}, \boldsymbol{\phi}) = \{(\theta_1, \phi_1), \ldots, (\theta_p, \phi_p)\}$, where $\theta \in [0, \pi]$ and $\phi \in [0, 2\pi)$ represent the elevation and azimuth angle, respectively. Moreover, assume that K snapshots are collected by the array. The element-space array output matrix $\mathbf{X} \in \mathbb{C}^{N \times K}$ is given by

$$\mathbf{X} = \mathbf{A}(\boldsymbol{\theta}, \boldsymbol{\phi})\mathbf{S} + \mathbf{N}, \tag{1}$$

where $\mathbf{A}(\boldsymbol{\theta}, \boldsymbol{\phi}) \in \mathbb{C}^{N \times P}$ represents the element-space steering vector matrix of a sensor array, $\mathbf{S} \in \mathbb{C}^{P \times K}$ is the signal matrix, and $\mathbf{N} \in \mathbb{C}^{N \times K}$ represents the measurement noise. The noise is assumed to be WSS, second-order ergodic, zero-mean, spatially and temporally white, circular complex Gaussian.

It is important to observe that in case of real-world arrays, the response to a far-field source is an unknown quantity that can only be estimated through calibration. Thus, in this paper we consider to have a discrete and noise corrupted version $\boldsymbol{\mathcal{A}}(\boldsymbol{\theta}_c, \boldsymbol{\phi}_c) \in \mathbb{C}^{N \times Q_e Q_a}$ of the array manifold, obtained by array measurements. In other words, we assume that the array manifold is *not* known explicitly (similarly to the case of real-world arrays). Here, $\boldsymbol{\theta}_c = [\theta_a, \ldots, \theta_{Q_e}]^T \in \mathbb{R}^{Q_e \times 1}$ and $\boldsymbol{\phi}_c = [\phi_a, \ldots, \phi_{Q_a}]^T \in \mathbb{R}^{Q_a \times 1}$ denote the measurement angles in elevation and azimuth, respectively.

III. MANIFOLD SEPARATION TECHNIQUE USING 2-D EADF

In this section we extend the Manifold Separation Technique (MST) [3], [4] by using the 2-D Effective Aperture Distribution Function (EADF), i.e. 2-D IDFT of the calibration data [3]. In particular, we express the array steering vector $\boldsymbol{a}(\theta, \phi) \in \mathbb{C}^{N \times 1}$ as the product of a sampling matrix and *two* Vandermonde vectors. Interestingly, the sampling matrix depends only on the sensor array

[*]This work was made possible by the Academy of Finland in the SMARAD Center of Excellence program.

[†]This work has been partially carried out while working at HUT.

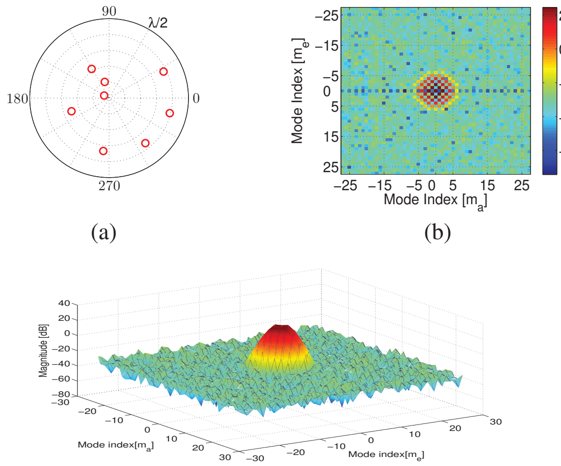

(a) (b)

(c)

Fig. 1. The geometry of the sensor array considered in this paper and the 2-D noisy EADF of the sensor with largest radius, are illustrated in (a) and (b)-(c), respectively. We assumed that the sensor array was calibrated at $Q_e = Q_a = 60$ points with SNR = 30 dB. The magnitude of the 2-D EADF is concentrated at $m_a = [-5, 5]$ and $m_e = [-5, 5]$.

configuration and its properties while the Vandermonde vectors depends only on the wavefield.

Here, we approximate the sampling matrix by the 2-D EADF. The 2-D EADF $\mathbf{G}_n \in \mathbb{C}^{(2Q_e-2)\times Q_a}$ for the nth sensor is defined as the 2-D IDFT of the corresponding nth *periodic* calibration matrix $\boldsymbol{\mathcal{A}}_n^{'}(\boldsymbol{\theta}, \boldsymbol{\phi}) \in \mathbb{C}^{(2Q_e-2)\times Q_a}$. Observe that the periodicity in both elevation and azimuth is a necessary condition for the computation of the 2-D IDFT. For the particular case of scalar wavefields, the periodic calibration matrix can be obtained as

$$\boldsymbol{\mathcal{A}}_n^{'}(\boldsymbol{\theta}, \boldsymbol{\phi}) = \begin{bmatrix} \boldsymbol{\mathcal{A}}_n(\boldsymbol{\theta}_c, \boldsymbol{\phi}_c) \\ \boldsymbol{\mathcal{A}}_n^r(\boldsymbol{\theta}_c, \boldsymbol{\phi}_c) \end{bmatrix}, \tag{2}$$

where $\boldsymbol{\mathcal{A}}_n^r(\boldsymbol{\theta}_c, \boldsymbol{\phi}_c)$ is obtained from $\boldsymbol{\mathcal{A}}_n(\boldsymbol{\theta}_c, \boldsymbol{\phi}_c)$ by a shift of 180° in azimuth and a flip in elevation, discarding the first and last row to avoid duplication of values at the poles of the sphere. Observe that expression (2) is different to the expressions for the vector-field version of the EADF introduced in [8].

Once the 2-D EADF for the N sensors are obtained, the steering vector can be modelled as

$$\boldsymbol{a}(\theta, \phi) = \boldsymbol{\Gamma}\mathbf{d}(\theta, \phi) + \boldsymbol{\varepsilon}(\mathcal{M}_e, \mathcal{M}_a), \tag{3}$$

where

$$\boldsymbol{\Gamma} = \begin{bmatrix} \mathrm{vec}\{\mathbf{G}_1\}^T \\ \vdots \\ \mathrm{vec}\{\mathbf{G}_N\}^T \end{bmatrix} \in \mathbb{C}^{N\times\mathcal{M}_e\mathcal{M}_a} \tag{4}$$

and

$$\mathbf{d}(\theta, \phi) = \mathbf{d}(\phi) \otimes \mathbf{d}(\theta) \in \mathbb{C}^{\mathcal{M}_e\mathcal{M}_a\times 1}. \tag{5}$$

It should be noticed that the quantity $\boldsymbol{\varepsilon}(\mathcal{M}_e, \mathcal{M}_a) \in \mathbb{C}^{N\times\mathcal{M}_e\mathcal{M}_a}$ represents the modelling errors due to truncation of the 2-D Fourier series representation of the array steering vector. Thus, $\boldsymbol{\varepsilon}(\mathcal{M}_e, \mathcal{M}_a)$ approaches zero as the number of modes $(\mathcal{M}_e, \mathcal{M}_a)$ increases. Observe also that $\mathrm{vec}\{\mathbf{G}_n\}$ stacks the matrix $\mathbf{G}_n$ into a column vector and $\otimes$ represents the Kronecker product. Moreover, $\mathbf{d}(\theta, \phi)$ is composed of the following Vandermonde structured vectors

$$\mathbf{d}(\theta) = [\mathrm{e}^{\mathrm{j}\frac{\mathcal{M}_e-1}{2}\theta}, \ldots, 1, \ldots, \mathrm{e}^{-\mathrm{j}\frac{\mathcal{M}_e-1}{2}\theta}]^T \in \mathbb{C}^{\mathcal{M}_e\times 1} \tag{6}$$

$$\mathbf{d}(\phi) = [\mathrm{e}^{\mathrm{j}\frac{\mathcal{M}_a-1}{2}\phi}, \ldots, 1, \ldots, \mathrm{e}^{-\mathrm{j}\frac{\mathcal{M}_a-1}{2}\phi}]^T \in \mathbb{C}^{\mathcal{M}_a\times 1}. \tag{7}$$

In Figure 1, the sensor array considered in this paper and a noisy 2-D EADF are illustrated. We have assumed that the array has been calibrated with SNR = 30 dB in $Q_e = Q_a = 60$ points. The saturation floor on the noisy 2-D EADF is due to the calibration noise. Moreover, it can be seen that the magnitude of the 2-D EADF is concentrated at $m_a = [-5, 5]$ and $m_e = [-5, 5]$.

IV. 2-D ROOT-MUSIC FOR ARBITRARY ARRAY CONFIGURATIONS

In this section, we show that by using the MST the 2-D MUSIC cost function for azimuth and elevation estimation can be reformulated as a bivariate polynomial, irrespective of the sensor array configuration. Then, in Section V we propose a rooting-based algorithm for joint azimuth and elevation estimation.

Let the element-space spatial covariance matrix (SCM) $\mathbf{R}_x \in \mathbb{C}^{N\times N}$ be given as

$$\mathbf{R}_x = \mathbf{A}(\boldsymbol{\theta}, \boldsymbol{\phi})\mathbf{R}_s\mathbf{A}(\boldsymbol{\theta}, \boldsymbol{\phi})^H + \sigma_\eta^2\mathbf{I}, \tag{8}$$

where $\mathbf{R}_s \in \mathbb{C}^{P\times P}$ is the signal covariance matrix. Writing $\mathbf{R}_x$ in terms of signal and noise subspaces and EVD we get

$$\mathbf{R}_x = \mathbf{E}_s\Lambda_s\mathbf{E}_s^H + \mathbf{E}_\eta\Lambda_\eta\mathbf{E}_\eta^H, \tag{9}$$

where $\mathbf{E}_s \in \mathbb{C}^{N\times P}$ and $\mathbf{E}_\eta \in \mathbb{C}^{N\times(N-P)}$ are the eigenvectors spanning the signal and noise subspaces, respectively. From equations (3), (8) and (9) we can easily obtain the 2D-MUSIC cost function

$$(\widehat{\theta}, \widehat{\phi}) = \arg\min_{\theta,\phi}\left\{\mathbf{d}(\theta, \phi)^H\boldsymbol{\Gamma}^H\mathbf{E}_\eta\mathbf{E}_\eta^H\boldsymbol{\Gamma}\mathbf{d}(\theta, \phi)\right\}. \tag{10}$$

Making the following substitutions $\zeta = \mathrm{e}^{\mathrm{j}\phi}, \omega = \mathrm{e}^{\mathrm{j}\theta}$, expression (10) can be equivalently given by the following *bivariate* polynomial

$$p(\zeta, \omega) = \mathbf{p}(\zeta)^T\mathbf{C}_b\mathbf{p}(\omega) = 0 \tag{11}$$

of degree $d_a = 2\mathcal{M}_a - 2$ in ζ and $d_e = 2\mathcal{M}_e - 2$ in ω. Here, $\mathbf{p}(\zeta) = [\zeta^{d_a}, \ldots 1]^T \in \mathbb{C}^{(d_a+1)\times 1}$ and $\mathbf{p}(\omega) = [\omega^{d_e}, \ldots 1]^T \in \mathbb{C}^{(d_e+1)\times 1}$. Note also that $\mathbf{C}_b \in \mathbb{C}^{(d_a+1)\times(d_e+1)}$ contains the coefficients of the bivariate polynomial. The bivariate polynomial in equation (11) can be seen as a univariate polynomial in ζ with coefficients which are univariate polynomials in ω. Observe that equation (11) simplifies to the ES-root-MUSIC [3] when θ is known.

The matrix $\mathbf{C}_b$, which contains the coefficients of the bivariate polynomial, can be obtained as

$$\mathbf{C}_b(d_a, d_e) = \sum\mathrm{diag}\left\{\sum\mathrm{diag}\left\{\boldsymbol{\Gamma}^H\mathbf{E}_\eta\mathbf{E}_\eta^H\boldsymbol{\Gamma}, d_a\right\}, d_e\right\}. \tag{12}$$

Here, $\sum\mathrm{diag}\{\cdot, d\}$ represents the sum of the (block) elements of the dth (block) diagonal. As an example, let us compute $\mathbf{C}_b(1, 1)$:

- Express the matrix $\boldsymbol{\Gamma}^H\mathbf{E}_\eta\mathbf{E}_\eta^H\boldsymbol{\Gamma}$ in block form

$$\boldsymbol{\Gamma}^H\mathbf{E}_\eta\mathbf{E}_\eta^H\boldsymbol{\Gamma} = \begin{bmatrix} \mathbf{C}_{1,1} & \ldots & \mathbf{C}_{1,\mathcal{M}_e} \\ \mathbf{C}_{2,1} & \ldots & \mathbf{C}_{2,\mathcal{M}_e} \\ \vdots & \ddots & \vdots \\ \mathbf{C}_{\mathcal{M}_e,1} & \ldots & \mathbf{C}_{\mathcal{M}_e,\mathcal{M}_e} \end{bmatrix} \tag{13}$$

and observe that $\sum\mathrm{diag}\{\boldsymbol{\Gamma}^H\mathbf{E}_\eta\mathbf{E}_\eta^H\boldsymbol{\Gamma}, 1\} = \mathbf{C}_{\mathcal{M}_e,1}$.

- Express the $\mathbf{C}_{\mathcal{M}_e,1}$ as

$$\mathbf{C}_{\mathcal{M}_e,1} = \begin{bmatrix} c_{1,1} & \dots & c_{1,\mathcal{M}_a} \\ c_{2,1} & \dots & c_{2,\mathcal{M}_a} \\ \vdots & \ddots & \vdots \\ c_{\mathcal{M}_a,1} & \dots & c_{\mathcal{M}_a,\mathcal{M}_a} \end{bmatrix} \quad (14)$$

and observe that $\sum \text{diag}\{\mathbf{C}_{\mathcal{M}_e,1}, 1\} = c_{\mathcal{M}_a,1}$.
- Thus, $\mathbf{C}_b(1,1) = c_{\mathcal{M}_a,1}$.

Equation (11) shows that the 2-D MUSIC cost function can be represented as a bivariate polynomial, *irrespective* of the sensor array configuration. However, the roots of bivariate polynomials *do not* constitute isolated points as in the univariate case. As claimed in [4], a simple rooting technique for azimuth and elevation estimation cannot be applied to (11). While this is generally true, in Section V we show that it is still possible to estimate azimuth and elevation angles via polynomial rooting, thus avoiding high complexity search-based techniques.

V. ES-PRIME FOR AZIMUTH AND ELEVATION ESTIMATION

In this section, we propose a rooting-based (polynomial complexity) algorithm for joint azimuth and elevation estimation on sensor arrays of arbitrary configurations, thus avoiding the spectral search-based 2-D MUSIC. The proposed Element-Space PRIME extends the PRIME [1] (Polynomial Rooting Intersection for Multidimensional Estimation) algorithm for Uniform Planar Arrays. Moreover, the proposed algorithm provides automatically paired estimates, avoiding the computationally complex pairing procedure proposed in [1].

Let us consider the bivariate polynomial in equation (11). In order to have unique solutions for (ζ, ω), we construct a system of two bivariate polynomial equations that vanish simultaneously for the roots which are related with the true sources. In particular, we decompose the noise subspace $\mathbf{E}_\eta$ into two orthogonal subspaces $\mathbf{E}_\eta^1$ and $\mathbf{E}_\eta^2$, such that

$$\mathbf{E}_\eta^1 \neq \mathbf{E}_\eta^2 \qquad \mathbf{E}_\eta^1 \cup \mathbf{E}_\eta^2 = \mathbf{E}_\eta. \quad (15)$$

Using the two orthogonal subspaces of the noise subspace, a system of bivariate polynomial equations that vanish simultaneously for the pair (ω, ζ) related with the DoA of the incoming signals, is given by

$$\begin{cases} g(\zeta, \omega) = \mathbf{p}(\zeta)^T \mathbf{C}_b^1 \mathbf{p}(\omega) = 0 \\ q(\zeta, \omega) = \mathbf{p}(\zeta)^T \mathbf{C}_b^2 \mathbf{p}(\omega) = 0, \end{cases} \quad (16)$$

where $\mathbf{C}_b^1$ and $\mathbf{C}_b^2$ are obtained from $\mathbf{\Gamma}^H \mathbf{E}_\eta^1 (\mathbf{E}_\eta^1)^H \mathbf{\Gamma}$ and $\mathbf{\Gamma}^H \mathbf{E}_\eta^2 (\mathbf{E}_\eta^2)^H \mathbf{\Gamma}$ in a similar way as $\mathbf{C}_b$.

Our goal now is to find the solutions for the system of bivariate polynomial equations in (16). There is a rich literature for computing roots of system of polynomials; see [9] and references therein. Since our main goal is to have a low computational complexity technique for computing the roots, we use a combination of multipolynomial resultants [9] and EVD for jointly estimate azimuth and elevation.

Let us consider the multipolynomial resultant formulation using the Sylvester matrix $\mathbf{S}(\omega) \in \mathbb{C}^{2d_a \times 2d_a}$ [1], whose structure is a double Toeplitz in ω. The multipolynomial resultant reduces the system of bivariate polynomial equations in (16) into the following system [9]

$$\mathbf{S}(\omega)\mathbf{u}(\zeta) = \mathbf{0}, \quad (17)$$

where $\mathbf{u}(\zeta) = [\zeta^{2d_a-1}, \dots, 1]^T \in \mathbb{C}^{2d_a \times 1}$. It can be shown that if (ω_0, ζ_0) is a solution of (16), $\mathbf{S}(\omega_0)$ is singular and $\zeta = \zeta_0$. This property is used to find the roots of the system of bivariate polynomial equations in (16).

In order to find the values of ω for which $\mathbf{S}(\omega)$ becomes singular, let us express $\mathbf{S}(\omega)$ as a matrix polynomial

$$\mathbf{S}(\omega) = \sum_{i=0}^{d_e} \mathbf{S}_i \omega^i. \quad (18)$$

The values for which $\mathbf{S}(\omega)$ becomes singular correspond to the roots of $\det\{\mathbf{S}(\omega)\}$, which in turn can be obtained from the generalized eigenvalues of the block companion matrix pencil $(\mathbf{C}_0, \mathbf{C}_1)$. More precisely, $\det\{\mathbf{S}(\omega)\} = \det\{\mathbf{C}_0 - \omega \mathbf{C}_1\}$, where $\mathbf{C}_0 \in \mathbb{C}^{2d_a d_e \times 2d_a d_e}$ and $\mathbf{C}_1 \in \mathbb{C}^{2d_a d_e \times 2d_a d_e}$ are given in [9].

Thus, the ω coordinates are found as the solutions of

$$\mathbf{C}_0 \mathbf{v} = \omega \mathbf{C}_1 \mathbf{v}. \quad (19)$$

Interestingly, if ω_1 is a generalized eigenvalue of $(\mathbf{C}_0, \mathbf{C}_1)$, the corresponding eigenvector has the form [9]

$$\mathbf{v}_1 = [\omega \mathbf{u}(\zeta), \dots \omega^{d_e} \mathbf{u}(\zeta)]^T \in \mathbb{C}^{2d_a d_e \times 1} \quad (20)$$

and the ζ_1 coordinate can be found as

$$\zeta_1 = \frac{\mathbf{v}_1(1)}{\mathbf{v}_1(2)}, \quad (21)$$

where $\mathbf{v}_1(n)$ represents the nth element of the vector $\mathbf{v}_1$.

Let $\boldsymbol{\psi} = [\boldsymbol{\omega} \quad \boldsymbol{\zeta}] \in \mathbb{C}^{2d_a d_e \times 2}$ represent the (paired) roots of (16), which were obtained from (19) and (21). The P roots which are related with the signals DoA are identified by selecting the ones with magnitude *simultaneously* closest to both (ω and ζ) unit circles.

As shown in [1], the error variance of the estimates provided by the PRIME algorithm, and consequently by the proposed ES-PRIME, do not attain the Cramér-Rao Lower Bound (CRLB). Thus, if statistical optimality is the goal, the computationally efficient MVP proposed next should be considered.

VI. MST-BASED MVP FOR AZIMUTH AND ELEVATION ESTIMATION

In this section, we reformulate the Weighted Subspace Fitting (WSF) [2] cost function for azimuth and elevation estimation using the MST (Section III). Moreover, we propose a computationally efficient MVP algorithm for the minimization of the novel cost function.

Let $\boldsymbol{\gamma} = [\boldsymbol{\theta}, \boldsymbol{\phi}]^T \in \mathbb{R}^{2P \times 1}$. The proposed MST-based WSF cost function for azimuth and elevation estimation is given by

$$f(\boldsymbol{\gamma}) = \text{Tr}\{\mathbf{\Pi}_{\Gamma D}^{\perp} \mathbf{E}_s \mathbf{W} \mathbf{E}_s^H\}, \quad (22)$$

where $\text{Tr}\{\cdot\}$ represents the trace operator and $\mathbf{W} = (\mathbf{\Lambda}_{\boldsymbol{s}} - \sigma_\eta^2 \mathbf{I})^2 \mathbf{\Lambda}_{\boldsymbol{s}}{}^{-1} \in \mathbb{C}^{P \times P}$. Moreover, $\mathbf{\Pi}_{\Gamma D}^{\perp}$ denotes the projection matrix to the orthogonal complement of $\mathbf{\Gamma}\mathbf{D}(\boldsymbol{\theta}, \boldsymbol{\phi})$, where $\mathbf{D}(\boldsymbol{\theta}, \boldsymbol{\phi}) = \mathbf{D}(\boldsymbol{\theta}) \diamondsuit \mathbf{D}(\boldsymbol{\phi})$ and $\diamondsuit$ represents the Khatri-Rao product.

The proposed MST-based MVP is a Newton-based method that minimizes (22) by iterating

$$\widehat{\boldsymbol{\gamma}}^{i+1} = \widehat{\boldsymbol{\gamma}}^{i} - \mu_i (\nabla^2 f(\boldsymbol{\gamma}))^{-1} \nabla f(\boldsymbol{\gamma}), \quad (23)$$

where $\mu_i < 1 \in \mathbb{R}$ is a coefficient used to adjust the step size in order to ensure convergence. In equation (23), $\nabla f(\boldsymbol{\gamma}) \in \mathbb{R}^{2P \times 1}$ represents the gradient and $\nabla^2 f(\boldsymbol{\gamma}) \in \mathbb{R}^{2P \times 2P}$ the approximate Hessian of the cost function. The expressions for the gradient and approximate Hessian are given by

$$\nabla f(\boldsymbol{\gamma}) = \begin{bmatrix} \nabla_{\boldsymbol{\theta}} f(\boldsymbol{\gamma}) \\ \nabla_{\boldsymbol{\phi}} f(\boldsymbol{\gamma}) \end{bmatrix} \quad (24)$$

and

$$\nabla^2 f(\boldsymbol{\gamma}) = \begin{bmatrix} \nabla^2_{\boldsymbol{\theta\theta}} f(\boldsymbol{\gamma}) & \nabla^2_{\boldsymbol{\theta\phi}} f(\boldsymbol{\gamma}) \\ \nabla^2_{\boldsymbol{\phi\theta}} f(\boldsymbol{\gamma}) & \nabla^2_{\boldsymbol{\phi\phi}} f(\boldsymbol{\gamma}) \end{bmatrix}. \quad (25)$$

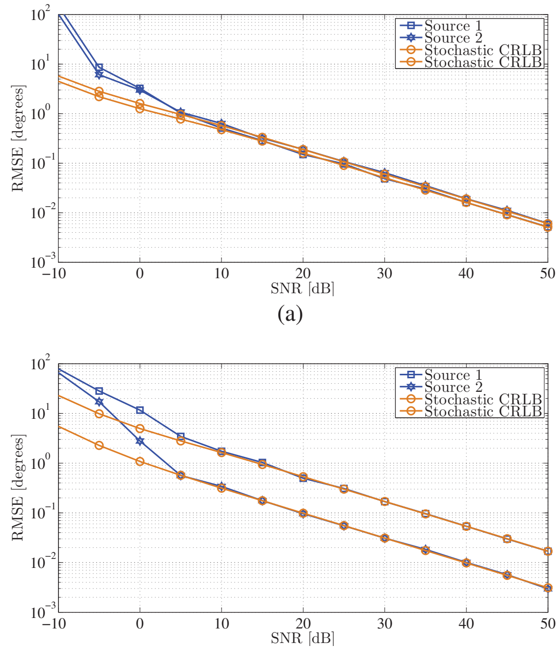

(a)

(b)

Fig. 2. Statistical performance of the proposed MST-based MVP for joint (a) elevation and (b) azimuth estimation when applied to the array given in Fig. 1, whose structure was not explicitly known. The initial estimates were obtained by the proposed ES-PRIME algorithm while the final estimate was obtained after 3 iterations of (23). The proposed algorithm attains the CRLB for both elevation and azimuth angles.

The gradient and each entry of the Hessian are found by substituting $(\mathbf{a} \leftrightarrow \boldsymbol{\phi}, \mathbf{a} \leftrightarrow \boldsymbol{\theta})$ and $(\mathbf{b} \leftrightarrow \boldsymbol{\phi}, \mathbf{b} \leftrightarrow \boldsymbol{\theta})$ into the following expressions

$$\nabla_{\mathbf{a}} f(\boldsymbol{\gamma}) = -2\Re\{\mathrm{diag}\{(\boldsymbol{\Gamma}\mathbf{D})^{\dagger}\mathbf{U}_s\mathbf{W}\mathbf{U}_s^H (\mathbf{I} - \boldsymbol{\Gamma}\mathbf{D}(\boldsymbol{\Gamma}\mathbf{D})^{\dagger})\boldsymbol{\Gamma}\dot{\mathbf{D}}_{\mathbf{a}}\}\} \tag{26}$$

$$\nabla^2_{\mathbf{ab}} f(\boldsymbol{\gamma}) = 2\Re\{[\dot{\mathbf{D}}_{\mathbf{b}}^H \boldsymbol{\Gamma}^H (\mathbf{I} - \boldsymbol{\Gamma}\mathbf{D}(\boldsymbol{\Gamma}\mathbf{D})^{\dagger})\boldsymbol{\Gamma}\dot{\mathbf{D}}_{\mathbf{a}}]^T \odot [(\boldsymbol{\Gamma}\mathbf{D})^{\dagger}\mathbf{U}_s\mathbf{W}\mathbf{U}_s^H((\boldsymbol{\Gamma}\mathbf{D})^{\dagger})^H]\}. \tag{27}$$

For the particular case of $(\mathbf{a} \leftrightarrow \boldsymbol{\theta})$, $\dot{\mathbf{D}}_{\boldsymbol{\theta}} = \dot{\mathbf{D}}(\boldsymbol{\theta})\diamondsuit\mathbf{D}(\boldsymbol{\phi})$ and $\dot{\mathbf{D}}(\boldsymbol{\theta}) = [\frac{\partial \mathbf{d}(\theta_1)}{\partial(\theta_1)}, \ldots, \frac{\partial \mathbf{d}(\theta_P)}{\partial(\theta_P)}] \in \mathbb{C}^{N \times P}$. Moreover, $\odot$ denotes the Schur-Hadamard product and $(\cdot)^{\dagger}$ represents the Moore-Penrose pseudo-inverse.

Unlike the conventional WSF [2], the proposed cost function (22) has information about the array non-idealities, making it more suitable for real-world arrays. Moreover, the proposed MST-based MVP yields significant computational benefits with respect to its conventional version [2], since we get closed-form expressions for the derivatives of the WSF cost function even in scenarios where only array calibration measurements is obtained (real-world sensor arrays). Further computational savings can be obtained by exploiting the inherent Vandermonde structure of the proposed MVP [10]. Notice that the initial value for the iterations in (23) should be "good enough" in order to avoid convergence to a local minimum instead of global optimum. The proposed rooting-based ES-PRIME should be the method of choice for the initial value.

VII. SIMULATION RESULTS

In this section we present simulation results illustrating the statistical performance of the proposed algorithms. We have assumed that two uncorrelated sources impinge the sensor array shown in Fig. 1(a) from $\{(\theta_1 = 10°, \phi_1 = 20°), (\theta_2 = 50°, \phi_2 = 40°)\}$ and that $K = 200$ snapshots were collected at the array output. This corresponds to a high-resolution scenario since the conventional beamformer is not able to resolve the DoAs. It is important to observe that the proposed algorithms only exploited the noisy calibration data of the sensor array, thus the array manifold was not explicitly known.

In Fig. 2, the statistical performance of the proposed MST-based MVP is shown. The RMSE was obtained after 500 independent Monte Carlo realizations. The initial estimates were obtained by the proposed ES-PRIME algorithm while the final estimate was obtained after 3 iterations of (23). The proposed algorithm shows a performance close to the CRLB in both elevation and azimuth.

VIII. CONCLUSIONS

In this paper two novel algorithms for elevation and azimuth estimation on arbitrary array configurations (possibly with imperfections) have been proposed. The proposed algorithms are based on the recently proposed MST. Unlike the search-based 2-D MUSIC, the proposed ES-PRIME jointly estimate elevation and azimuth with *polynomial* complexity. The proposed MST-based MVP is also a computationally efficient algorithm (wrt the conventional MVP) due to the convenient expressions for the derivatives of the WSF cost function and Vandermonde structure. We have applied the algorithms to a sensor array of arbitrary configuration (whose structure was not explicitly known) and shown that the proposed MST-based MVP attains the CRLB.

IX. REFERENCES

[1] G. F. Hatke and K. W. Forsythe, "A class of polynomial rooting algorithms for joint azimuth/elevation estimation using multidimensional arrays," in *Asilomar Conference on Signals, Systems and Computers*, 1995, vol. 1, pp. 694–699.

[2] M. Viberg, B. Ottersten, and T. Kailath, "Detection and estimation in sensor arrays using weighted subspace fitting," *IEEE Trans. Signal Processing*, vol. 39, no. 11, pp. 2436–2449, November 1991.

[3] F. Belloni, A. Richter, and V. Koivunen, "DoA estimation via manifold separation for arbitrary array structures," *IEEE Trans. Signal Processing*, vol. 55, no. 10, pp. 4800–4810, October 2007.

[4] M. A. Doron and E. Doron, "Wavefield modeling and array processing, part II - algorithms," *IEEE Trans. Signal Processing*, vol. 42, no. 10, pp. 2560–2570, October 1994.

[5] M. Pesavento and J. F. Böhme, "Eigenstructure-based azimuth and elevation estimation in sparse uniform rectangular arrays," in *Workshop on Sensor Array and Multichannel Signal Processing*, 2002, pp. 327–331.

[6] J. Li, P. Stoica, and D. Zheng, "An efficient algorithm for two-dimensional frequency estimation," *Muldimensional Systems and Signal Processing*, vol. 7, pp. 151–178, 1996.

[7] B. Friedlander, "The root–MUSIC algorithm for direction finding with interpolated arrays," *Signal Processing*, vol. 30, pp. 15–19, 1993.

[8] M. Landmann, A. Richter, and R. S. Thoma, "DoA resolution limits in MIMO channel sounding," in *International Symposium on Antennas and Propagation and USNC/URSI National Radio Science Meeting*, 2004.

[9] D. Manocha, "Solving systems of polynomial equations," *IEEE Computer Graphics and Applications*, vol. 14, no. 2, pp. 46–55, 1994.

[10] J. Selva, "An efficient newton-type method for the computation of ML estimators in a uniform linear array," *IEEE Trans. Signal Processing*, vol. 53, no. 6, pp. 2036–2045, June 2005.